LASER INTERFEROMETER GRAVITATIONAL WAVE OBSERVATORY
- LIGO -
CALIFORNIA INSTITUTE OF TECHNOLOGY
MASSACHUSETTS INSTITUTE OF TECHNOLOGY

Technical Note **LIGO-T22xxxxx–** 2022/07/13

2022 LIGO SURF Interim Report 1: Emissivity Engineering for Radiative CryoCooling

Clare Nelle

California Institute of Technology
LIGO Project, MS 18-34
Pasadena, CA 91125
Phone (626) 395-2129
Fax (626) 304-9834
E-mail: info@ligo.caltech.edu

Massachusetts Institute of Technology
LIGO Project, Room NW22-295
Cambridge, MA 02139
Phone (617) 253-4824
Fax (617) 253-7014
E-mail: info@ligo.mit.edu

LIGO Hanford Observatory
Route 10, Mile Marker 2
Richland, WA 99352
Phone (509) 372-8106
Fax (509) 372-8137
E-mail: info@ligo.caltech.edu

LIGO Livingston Observatory
19100 LIGO Lane
Livingston, LA 70754
Phone (225) 686-3100
Fax (225) 686-7189
E-mail: info@ligo.caltech.edu

http://www.ligo.caltech.edu/

Contents

1 Introduction/Motivation

Since the LIGO-VIRGO Scientific Collaboration's detection of gravitational waves in 2016, the field of gravitational wave astronomy has allowed for new ways to observe the physical phenomena. Collaborators hope to refine the precision of LIGO detection with further Advanced LIGO upgrades to explore new avenues in gravitational wave astronomy and multimessenger astrophysics. The LIGO Voyager version is an upgrade that will increase the sensitivity to about 700-1100 Mpc [**1**] by using cryogenic temperatures of 123 K to reduce thermal noise within the LIGO barrel. Constacio et. al. found that silicon has a high enough natural emissivity to maintain the temperature of test masses at 123K, meaning that it is an appropriate material to use in the Voyager upgrade barrel [**2**]. However, because the LIGO interferometer lasers must be very powerful (around 10W), Constacio et. al. theorized that the barrel will also require a high thermal emissivity to increase radiative coupling to its cooled environment. This will improve the cool-down time of the Voyager upgrade apparatus and help maintain the system at 123 K despite the excess heating from the laser [**2**].

Constancio et. al. showed that high emissivity coating is necessary if the laser power is greater than 6W. Therefore, it is important to test the emissivities of various materials in order to identify coatings that will sufficiently increase coupling from the excess power from the interferometer laser. The coatings will need to have emissivity between 10 - 100 um wavelength [**3**]. This will reduce the cool-down time of the system and allow for conditions to hold the system at 123K.

To determine the emissivities of various black coatings, the cool-down curves from room temperature to 123 K is monitored with respect to time using thermocouple thermometers for test masses in a cryostat chamber held at vacuum. Then, the emissivity value and propagated uncertainty can be extracted from these data by plotting emissivity against temperature [**2**]. Obtaining these data is an expensive and time-consuming process, and therefore it is beneficial to optimize this procedure and model to efficiently obtain emissivity values while minimizing uncertainty. By simulating different geometries and materials, it is possible to find a model with the lowest noise in the data by tracking how errors propagate using Markov Chain Monte Carlo (MCMC) analysis. This optimal experimental design can be applied to emissivity tests for many black coatings that can potentially be used in the LIGO Voyager upgrade.

2 Progress

To meet the outlined proposals, it was important to learn about how to implement MCMC for parameter estimation, refine our current model of heat transfer within the cryostat by improving the view factor calculation between the test mass and holes in the shield, and calibrate the Resistance Temperature Detectors (RTDs) in the cryostat chamber along with other laboratory work.

2.1 Learning to Use MCMC

To simulate the experimental designs and geometries in python and use MCMC analysis to observe how simulated uncertainty propagates, it was important to develop a knowledge of the python module emcee and the basics of Bayesian statistics. A qualitative summary of MCMC is described in Figure 1. The next step was to implement the python module emcee to fit a simple linear model with Gaussian noise to learn how MCMC is used in python. Matt Pitkin's linear model tutorial helped develop an understanding of how to create uniform and Gaussian priors and how to debug helper functions [**5**]. Next, I used a simulated parabolic dataset, implementing three parameters. This helped develop an understanding of how the prior distributions effect the movement of walkers over the parameter vector space. Figure 2 shows the simulated data, trace plots, and corner plot for fitting a parabolic curve. These simple models will provide the structure to build the more complex model for the cool down curve of the cryostat's test mass.

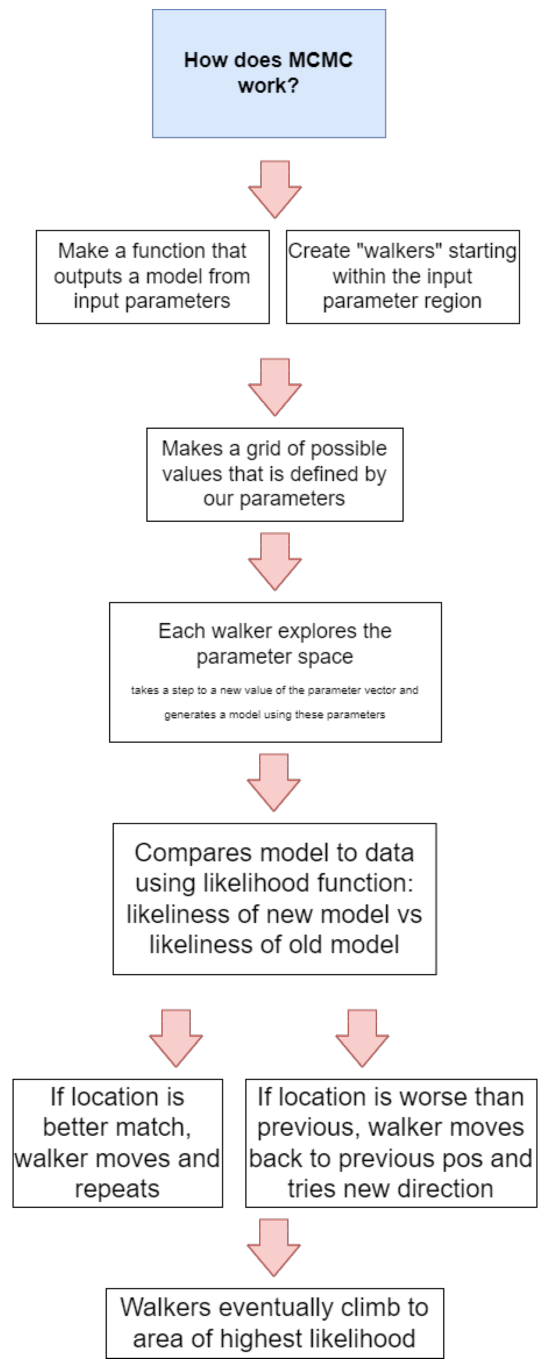

Figure 1: A qualitative understanding of the MCMC process helps build a foundation for understanding and implementing the emcee package.

2.2 Refining the View Factor Estimation for Heat Leaks

Heat leaks in the inner shield cause some thermal energy to leave the system via radiative heat transfer. The model implements a geometry of radiative heat transfer between the test mass wafer and a circular hole in the shield. The current model for heat transfer within the cryostat uses a geometry with the test mass represented as a disk on the same plane as the hole in the shield, providing an upper bound for the fraction of radiation that is leaking through the hole (Figure 3). However, the simulation can be made more precise by implementing an equation for the view factor of the test mass and a hole in the shield where the test mass is on a perpendicular plane to the shield because it more accurately represents the geometry of the cryostat. This aspect of the model can be

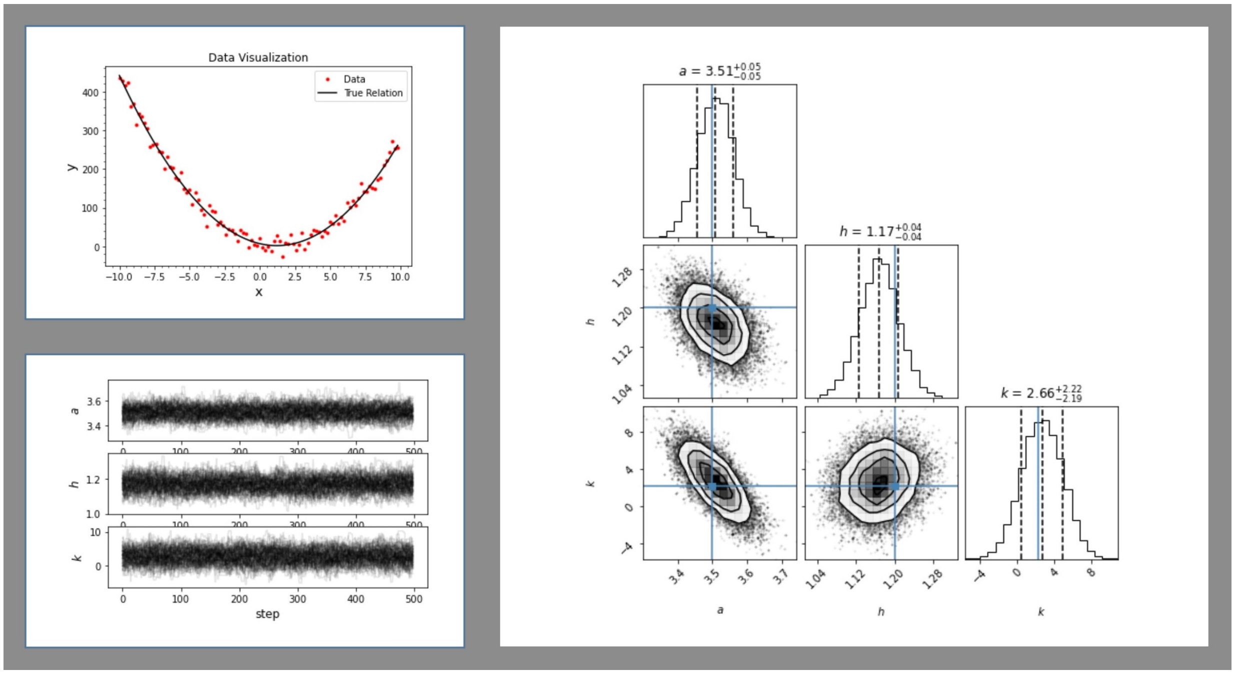

Figure 2: *Top Left:* The simulated data was a parabola with parameters in the form $y = a(x - h) + k$ with random noise. *Bottom Left:* Trace plots were a useful indicator for how well the walkers were exploring the parameter space. *Right:* The generated corner plots provide information on the covariance between the parameters. It is also useful to see how the walkers converged.

refined by implementing an equation for the view factor of two rectangles on perpendicular planes. Although the test mass is a disk, the view factor can still be approximated using this geometry.

This updated model for the net radiative heat transfer of the heat leaks and the sample was developed by first understanding differential equation estimation through the python library scipy method solve_ivp. A simple model

$$mc_p\frac{dT}{dt} = \frac{kA}{l}T$$

for heat conduction of a metal rod with cross sectional area A, length l, and the material's thermal conductivity k, was used to plot the temperate at one end of a rod as a function of time if the other end of the rod was cooled or heated to a certain value.

In addition, a model using the net radiative heat transfer equation with the updated view factor was implemented into the solve_ivp function. This equation is very similar to the conductive heat transfer, it is a differential equation equal to constants multiplied by the fourth powers of the temperature difference instead of the first powers in conductive heat transfer. This means that the solution to an initial value problem for net radiative heat transfer is also a decaying exponential. Figure 4 shows how changing the view factor influences the cooldown time. Model for radiative heat transfer:

$$mc_p\frac{dT_1}{dt} = \frac{\sigma(T_2^4 - T_1^4)}{(\frac{1-\epsilon_1}{A_1\epsilon_1} + \frac{1}{A_1F} + \frac{1-\epsilon_2}{A_2\epsilon_2})}$$

where A_1, A_2 and ϵ_1, ϵ_2 are the surface areas of the test mass/heat leak and the emissivities respectively. The denominator can be thought of as an analogy of the resistors whose strength are related to the surface emissivities and the orientation of the surfaces [**4**].

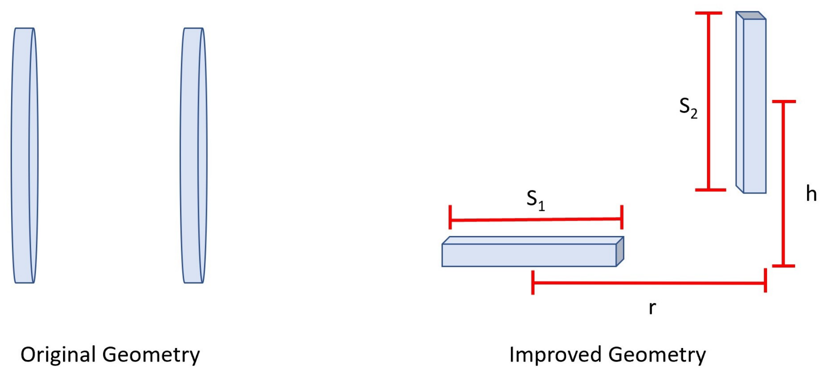

Figure 3: A visualization of the improved view factor geometry (RHS).

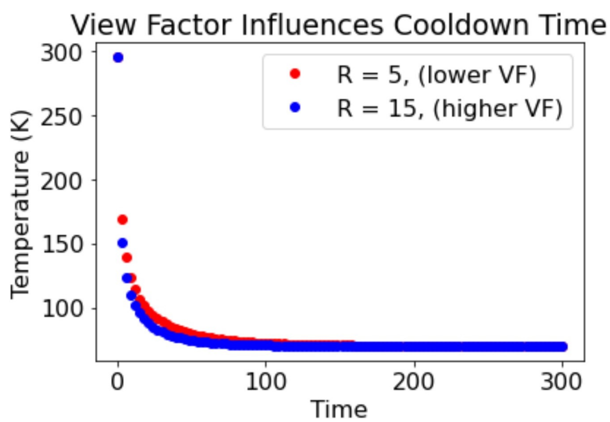

Figure 4: The graph depicts the cool down curve of a simulated geometry in Figure 3. It gives the temperature of the second mass with side length S_2 as a function of time. This example shows what happens when S_2 is scaled by a factor of ten, meaning that the view factor increases and the value of A_2 increases. This slows the rate of heat transfer and increases the cooldown time for any arbitrary temperature.

2.3 Calibrating RTDs/Cryostat Cooldown

In a previous cooldown, the RTD measuring the inner shield was reading colder temperatures than the RTD on the cold head. This is physically impossible, leading the the belief that the RTDs were inaccurate relative to each other. This prompted recalibration of the RTDs. For each RTD, the resistance was measured using a digital multimeter at the freezing point of water and at the boiling point of Nitrogen. From these two measurements, a linear fit line would give the temperature as a function of resistance for each RTD. Two measurements of the resistance across each RTD was measured. Only one measurement in the liquid nitrogen bath was used because the boiling point of nitrogen is much lower than room temperature, meaning that the temperature of the liquid nitrogen is known to high certainty. From initial observations, the RTD that was previously attached to the outer shield was reading a slightly higher resistance at the liquid nitrogen measurement than the other RTDs.

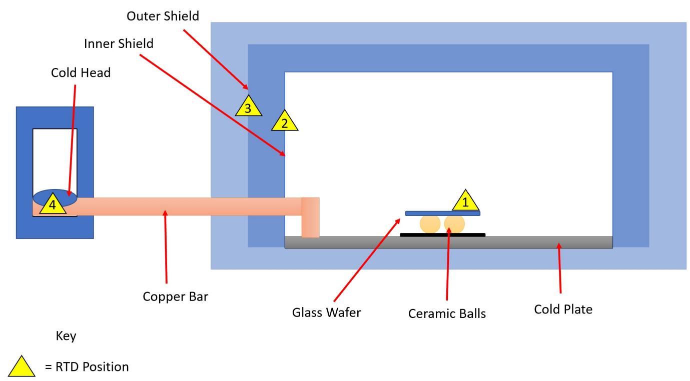

Figure 5: The cross-sectional diagram of the cryostat helps with a basic understanding of the system. This was necessary to understand when taking apart the cryostat and removing the RTDs, but it is also necessary for a qualitative understanding when building a model of this system in python. RTD 2 was the sensor that was previously reading temperatures that were physically impossible. There is not currently an RTD 4 on the cold head because it is broken.

Other work to assist in a cooldown of the cyryostat was completed, including preparing the glass wafer. This will be useful when taking data for multiple samples in the upcoming weeks.

3 Challenges

3.1 MCMC

Understanding MCMC both in terms of statistics and with the implementation of emcee has been challenging. It is not yet clear why some of the parabolic simulations do not create corner plots with enough data points (increasing or decreasing the burn-in has no effect), but it is theorized that this happens when the priors are too close to physically impossible bounds. This will be something that I continue to learn about as I progress with emcee.

3.2 Improving View Factor Estimation

Although the new view factor estimation is more accurate than the parallel planes geometry that was previously implemented, it is not a true representation of cryostat geometry because the test mass is a disk. Deriving view factors in this geometry is very challenging and involved and therefore I used tables with previously derived equations for common geometries [**6**]. This is an improvement, but not an accurate representation of the experimental conditions.

3.3 RTD Calibration

During the calibration process, two RTDs were broken because the RTD wires were spread apart with the alligator clips to dip them in the ice bath or liquid nitrogen. This means that there is no RTD reading the temperature of the cold head. Figure 5 shows the positions of the RTDs. Position 4 is missing an RTD at this time. This problem can be avoided by taping the alligator clips together.

4 Future Work

- Implement emcee to observe how simulated uncertainty propagates in simulated cryostat geometries. This will require creating a more complex model with multiple priors as well as implementing the work done to build simple radiative heat transfer models using scipy. Because the running code to solve a differential equation will be time consuming and will have to be iterated for every walker and their steps, it will be necessary to increase the efficiency of both emcee and the differential equation solver. This could be a challenging problem to solve because it will involve understanding new documentation again.
- In the lab, new RTDs will need to be calibrated. The glass wafer cooldown has also prepared us to carry out more cooldowns with different substances in the chamber.

5 Acknowledgments

Thank you to Professor Rana Adhikari (Experimental Gravitational Physics, LIGO Lab Caltech) and Radhika Bhatt (graduate student, Adhikari research group) for their support in this project as mentors. I also appreciate and acknowledge the National Science Foundation Research Experience for Undergraduates program, the California Institute of Technology, and the LIGO Summer Undergraduate Research Fellowship for this opportunity.

References

[1] V. Mitrofanov, *LIGO Voyager Project of Future Gravitational Wave Detector*, https://dcc.ligo.org/public/0139/G1602258/002/Presentation_Mitrofanov.pdf.

[2] M. Constancio and R. X. Adhikari and O. D. Aguiar and K. Arai and A. Markowitz and M. A. Okada and C. C. Wipf, International Journal of Heat and Mass Transfer, **157**, 2020.

[3] R. X Adhikari, A. Brooks, B. Shapiro, D. McClelland, E. K. Gustafson, V. Mitrofanov, K. Arai, C. Wipf, *LIGO Voyager Project of Future Gravitational Wave Detector*, https://docs.ligo.org/voyager/voyagerwhitepaper/main.pdf.

[4] Y. A. Cengel, Heat transfer: a practical approach, McGraw-Hill series in mechanical engineering (McGraw-Hill, 2003) Chap. 12.

[5] M. Pitkin, An example using emcee, 2018, Accessed: 7-11-2022, Available: http://mattpitkin.github.io/samplers-demo/pages/emcee/

[6] I. Martinez, Radiative View Factors, (http://webserver.dmt.upm.es/ isidoro/tc3/Radiation %20View%20factors.pdf)

[7] The ideas for this report were based off of discussions with Professor Rana Adhikari (Experimental Gravitational Physics, LIGO Lab Caltech), Radhika Bhatt (graduate student, Adhikari research group) and LIGO SURF student, Hiya Gada.